

Critical Regions for Activation Gating of the Inositol 1,4,5-Trisphosphate Receptor*

Received for publication, January 21, 2003, and in revised form, March 4, 2003
Published, JBC Papers in Press, March 5, 2003, DOI 10.1074/jbc.M300646200

Keiko Uchida‡§, Hiroshi Miyauchi¶||, Teiichi Furuichi**, Takayuki Michikawa‡ §§, and Katsuhiko Mikoshiba‡ §§¶||

From the ‡Division of Molecular Neurobiology, Department of Basic Medical Science, Institute of Medical Science, University of Tokyo, 4-6-1 Shirokanedai, Minato-ku, Tokyo 108-8639, Japan, the §Department of Pediatrics, Keio University School of Medicine, 35 Shinanomachi, Shinjuku-ku, Tokyo 160-8582, Japan, the ¶Department of Neurosurgery, Japanese Red Cross Medical Center, 4-1-22 Hiro-o, Shibuya-ku, Tokyo 150-8935, Japan, the ||Department of Neurosurgery, University of Tokyo, 7-3-1 Hongo, Bunkyo-ku, Tokyo 113-8655, Japan, the Laboratories for **Molecular Neurogenesis and §§Developmental Neurobiology, Brain Science Institute, RIKEN, 2-1 Hirosawa, Wako, Saitama 351-0198, Japan, and the ‡‡Calcium Oscillation Project, International Cooperative Research Project, Japan Science and Technology Corporation, 3-4-4, Shirokanedai, Minato-ku, Tokyo 108-0071, Japan

To understand the molecular mechanism of ligand-induced gating of the inositol 1,4,5-trisphosphate (IP₃) receptor (IP₃R)/Ca²⁺ release channel, we analyzed the channel properties of deletion mutants retaining both the IP₃-binding and channel-forming domains of IP₃R1. Using intrinsically IP₃R-deficient cells as the host cells for receptor expression, we determined that six of the mutants, those lacking residues 1–223, 651–1130, 1267–2110, 1845–2042, 1845–2216, and 2610–2748, did not exhibit any measurable Ca²⁺ release activity, whereas the mutants lacking residues 1131–1379 and 2736–2749 retained the activity. Limited trypsin digestion showed that not only the IP₃-gated Ca²⁺-permeable mutants lacking residues 1131–1379 and 2736–2749, but also two nonfunctional mutants lacking residues 1–223 and 651–1130, retained the normal folding structure of at least the C-terminal channel-forming domain. These results indicate that two regions of IP₃R1, *viz.* residues 1–223 and 651–1130, are critical for IP₃-induced gating. We also identified a highly conserved cysteine residue at position 2613, which is located within the C-terminal tail, as being essential for channel opening. Based on these results, we propose a novel five-domain structure model in which both N-terminal and internal coupling domains transduce ligand-binding signals to the C-terminal tail, which acts as a gatekeeper that triggers opening of the activation gate of IP₃R1 following IP₃ binding.

Inositol 1,4,5-trisphosphate (IP₃)¹ is a second messenger that is produced by hydrolysis of phosphatidylinositol 4,5-bisphosphate in response to activation by extracellular stimuli of the G protein- or tyrosine kinase-coupled receptors on the plasma membrane in various cell types (1). IP₃ mediates the release of Ca²⁺ from intracellular storage sites such as the endoplasmic reticulum by binding to the IP₃ receptor (IP₃R)/Ca²⁺ release channel. IP₃-induced Ca²⁺ release (IICR) regulates numerous

physiological processes, including fertilization, cell proliferation, development, muscle contraction, secretion, learning, and memory. In this signal transduction pathway, the IP₃R works as a switch that converts the information carried by extracellular stimuli into intracellular Ca²⁺ signals.

IP₃-gated intracellular Ca²⁺ release channels are composed of four IP₃R subunits (2). There are at least three types of IP₃Rs (IP₃R1, IP₃R2, and IP₃R3) (3), and they exist as both homo- and heterotetramers (4). The structure of IP₃Rs has traditionally been divided into three functional domains (3, 5): the N-terminal ligand-binding domain; the modulatory/coupling domain; and the C-terminal transmembrane/channel-forming domain, which contains six putative membrane-spanning regions. The transmembrane region is required for the intermolecular interaction in the formation of a tetrameric complex (6–9), and it is likely that the C-terminal cytoplasmic region just following the putative membrane-spanning regions has a supportive role in the association among the subunits (6, 9). An ion conduction pore has been proposed to be located in the hydrophobic segment between the fifth and sixth transmembrane regions (10, 11). The primary sequence of the transmembrane domain adjacent to the pore-forming segment is highly homologous to that of the ryanodine receptor (RyR), another type of intracellular Ca²⁺ release channel, suggesting that these two channels might share a common structure for the conduction of Ca²⁺ ions.

Each IP₃R subunit has a single high affinity IP₃-binding site (2). The IP₃-binding core, a minimum essential region for specific IP₃ binding (12), resides among residues 226–578 of mouse IP₃R1 (2749 amino acids) (13), and it contains 11 essential basic amino acids for IP₃ binding (14). The N-terminal 225 residues, which are close to the IP₃-binding core, have been thought to function as a suppressor for IP₃ binding because their deletion from the N-terminal 734-amino acid region results in significant enhancement of IP₃-binding activity (12, 15). IICR is a positively cooperative process (16–18), *i.e.* the binding of at least two IP₃ molecules to a single tetrameric IP₃R channel is required for channel opening. IP₃ binding elicits a large conformational change in the N-terminal cytoplasmic portion of the IP₃R (19). Furthermore, the C-terminal cytoplasmic region following the transmembrane domain is thought to be involved in the IP₃-induced gating of the receptor because monoclonal antibody (mAb) 18A10, whose epitope is located in the C-terminal portion of mouse IP₃R1 (13, 20, 21), has an inhibitory effect on IICR, without causing any decrease in the

* This work was supported by grants from the Ministry of Education, Science, Sports, and Culture of Japan. The costs of publication of this article were defrayed in part by the payment of page charges. This article must therefore be hereby marked “advertisement” in accordance with 18 U.S.C. Section 1734 solely to indicate this fact.

¶¶ To whom correspondence should be addressed. Tel.: 81-3-5449-5316; Fax: 81-3-5449-5420; E-mail: mikosiba@ims.u-tokyo.ac.jp.

¹ The abbreviations used are: IP₃, inositol 1,4,5-trisphosphate; IP₃R, IP₃ receptor; IICR, IP₃-induced Ca²⁺ release; RyR, ryanodine receptor; mAb, monoclonal antibody.

affinity of the receptor for IP_3 (21). Controlled trypsinization induces fragmentation of mouse IP_3R1 into five major fragments, and all four N-terminal cytoplasmic fragments, which contain the IP_3 -binding core, are associated directly or indirectly with the remaining C-terminal fragment, which contains the channel domain (22). The trypsinized IP_3R retains significant IICR activity, indicating that intramolecular interaction within a subunit and/or intermolecular interaction between neighboring subunits could effect functional coupling between IP_3 binding and channel opening (22). However, the sites of the interfaces between the cytoplasmic fragments and the channel domain and the molecular mechanism of their coupling remain to be elucidated.

IICR has been shown to occur in a quantal manner in permeabilized cells and isolated endoplasmic reticulum membranes (23, 24). The addition of submaximal concentrations of IP_3 in the presence of Ca^{2+} pump inhibitors leads to the partial release of sequestered Ca^{2+} , and the amount of released Ca^{2+} varies with the concentration of IP_3 (24). Although the Ca^{2+} release terminates abruptly, because it can be reinitiated by an additional increment in IP_3 concentration (24), the rapid termination of Ca^{2+} release is not due to ordinary inactivation or desensitization of the receptor. Purified IP_3Rs reconstituted into lipid vesicles reveal a quantal Ca^{2+} flux (17, 25), indicating that the quantal release of Ca^{2+} is an intrinsic property of the IP_3R . Similar behavior was observed for the RyR, which mediates Ca^{2+} -induced Ca^{2+} release from intracellular Ca^{2+} stores (26), but has not been observed for other ligand-gated ion channels on the plasma membrane, suggesting that the quantal release is a fundamental and unique property of the intracellular Ca^{2+} release channels.

To understand the molecular basis of the ligand-induced gating of the IP_3R , we analyzed a series of internal deletion mutants and site-directed mutants of mouse IP_3R1 expressed in intrinsically IP_3R -deficient R23-11 cells (27). We found that at least two regions and a cysteine residue are essential for IP_3 -dependent gating of IP_3R1 . These findings provide us with new insight into the gating mechanism of the IP_3R .

EXPERIMENTAL PROCEDURES

Plasmid Constructions—For transfection of mouse wild-type IP_3R1 cDNA, pBact-STneoB-C1 (28) was used. Seven deletion mutant cDNAs of mouse IP_3R1 , D651–1130, D1131–1379, D1267–2110, D1692–1731, D1845–2042, D1845–2216, and D2610–2748 (6), were subcloned into pAneo (27) at the *SalI* sites. To construct D1–223, an *XhoI* site was introduced at nucleotide 998 of mouse IP_3R1 by PCR using green fluorescent protein-fused IP_3R -D223² as the template DNA. An *XhoI*-*KpnI* fragment isolated from green fluorescent protein-fused IP_3R -D223 was ligated to a *SalI*-*KpnI* fragment of pBact-STneoB-C1. The resultant plasmid, pBact-STneoB-D1–223, uses nucleotides 998–1000, which correspond to an intrinsic methionine residue at position 224, as a start codon (ATG) for transcription. To construct D2736–2749, a *KpnI*-*XhoI* fragment isolated from enhanced green fluorescent protein-fused $IP_3R/\Delta 18A10$ (29) was ligated to a *KpnI*-*SalI* fragment of pBact-STneoB-C1. To substitute serine for cysteine at position 1976, 2610, or 2613 or at both positions 2610 and 2613 of mouse IP_3R1 , site-directed mutagenesis was performed with a MutanK kit (Takara) using primers containing the appropriate substitutions (5'-GTGGTTTTCAGACAGCAGCTG-3' for nucleotides 6245–6265, 5'-CAGATGAAGCTCGTGGTTTTT-3' for nucleotides 8146–8166, 5'-TTCCAAGCCGGAGATGAAGCA-3' for nucleotides 8156–8176, and 5'-AAGCCGGAGATGAAGCTCGTGGT-3' for nucleotides 8150–8172). The *EcoRI* fragment from the *EcoRI* site (nucleotide 6979) internal to the 3'-end of the mouse IP_3R1 isolated from pBactS-C1 (13) was subcloned into pBluescript SK(+). The *BamHI* fragment (2532 bp) of the mouse IP_3R1 isolated from pBactS-C1 (13) was subcloned into pUC118. These plasmids were used as template DNAs. After the mutated *EcoRI* or *BamHI* fragments were put back

into pBactS-C1, the mutated cDNAs were subcloned into pBact-STneoB (28) at the *SalI* sites. All PCR products and mutations were confirmed by DNA sequencing.

Generation of Wild-type and Deletion Mutant IP_3R1 -expressing Cell Lines—R23-11 cells (27) were cultured in RPMI 1640 medium supplemented with 10% fetal calf serum, 1% chicken serum, 50 μ M 2-mercaptoethanol, 4 mM glutamine, 100 units/ml penicillin, and 100 μ g/ml streptomycin at 39.5 °C in 5% CO_2 . Expression plasmids were linearized and transfected into R23-11 cells by electroporation as previously described (27) or by lipofection (Effectene, QIAGEN Inc.).³ Several stable clones were selected in medium containing 2 mg/ml G418 (Sigma) ~7–10 days after transfection. Expression of the IP_3R and its mutants was confirmed by immunoblotting with mAbs 4C11 and/or 18A10 using cell lysates boiled in SDS-PAGE sample buffer (5 mM EDTA, 50 mM Tris-HCl, pH 6.8, 100 mM dithiothreitol, 2% SDS, and 10% glycerol). Immunoblot analysis was performed as described previously (22).

Preparation of Membrane Fractions from Stable Cells Expressing Mouse IP_3R1 and Its Mutants—Membrane fractions were prepared in accordance with the protocol for mouse cerebella described by Michikawa *et al.* (18), with minor modifications. Cells were collected by centrifugation, washed twice with cold phosphate-buffered saline, and homogenized in ice-cold homogenization buffer (5 mM NaN_3 , 0.1 mM EGTA, 1 mM 2-mercaptoethanol, and 20 mM HEPES-NaOH, pH 7.4) containing protease inhibitors (0.1 mM phenylmethylsulfonyl fluoride, 10 μ M leupeptin, 10 μ M pepstatin A, and 10 μ M E-64) by 40 strokes in a chilled glass-Teflon Potter homogenizer at 1000 rpm. The homogenate was centrifuged at $1100 \times g$ for 10 min at 2 °C. The supernatant was centrifuged at $100,000 \times g$ in a Beckman TLA100.3 rotor for 30 min at 2 °C. The pellet was resuspended in an appropriate volume of wash buffer (600 mM KCl, 5 mM NaN_3 , 20 mM $Na_4P_2O_5$, 1 mM 2-mercaptoethanol, and 10 mM HEPES-HCl, pH 7.2) containing protease inhibitors. The suspension was centrifuged at $1100 \times g$ for 10 min, and the supernatant was centrifuged at $63,000 \times g$ for 30 min at 2 °C. The pellet was finally suspended in an appropriate volume of Ca^{2+} release buffer (110 mM KCl, 10 mM NaCl, 5 mM KH_2PO_4 , 1 mM 2-mercaptoethanol, and 50 mM HEPES-KOH, pH 7.2) containing protease inhibitors to a final concentration of ~15 mg/ml protein. Ca^{2+} release buffer was passed over Chelex 100 (Bio-Rad) to eliminate any extra free Ca^{2+} before use. The membrane fractions were either used immediately or frozen in liquid nitrogen and stored at –80 °C until used.

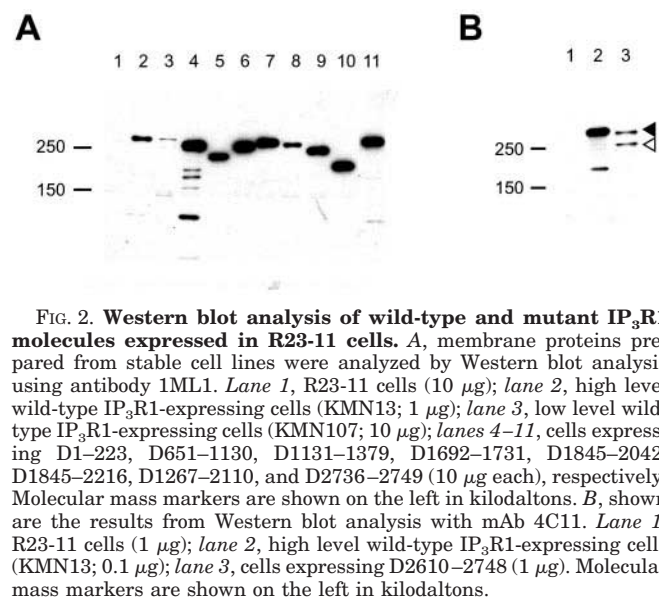
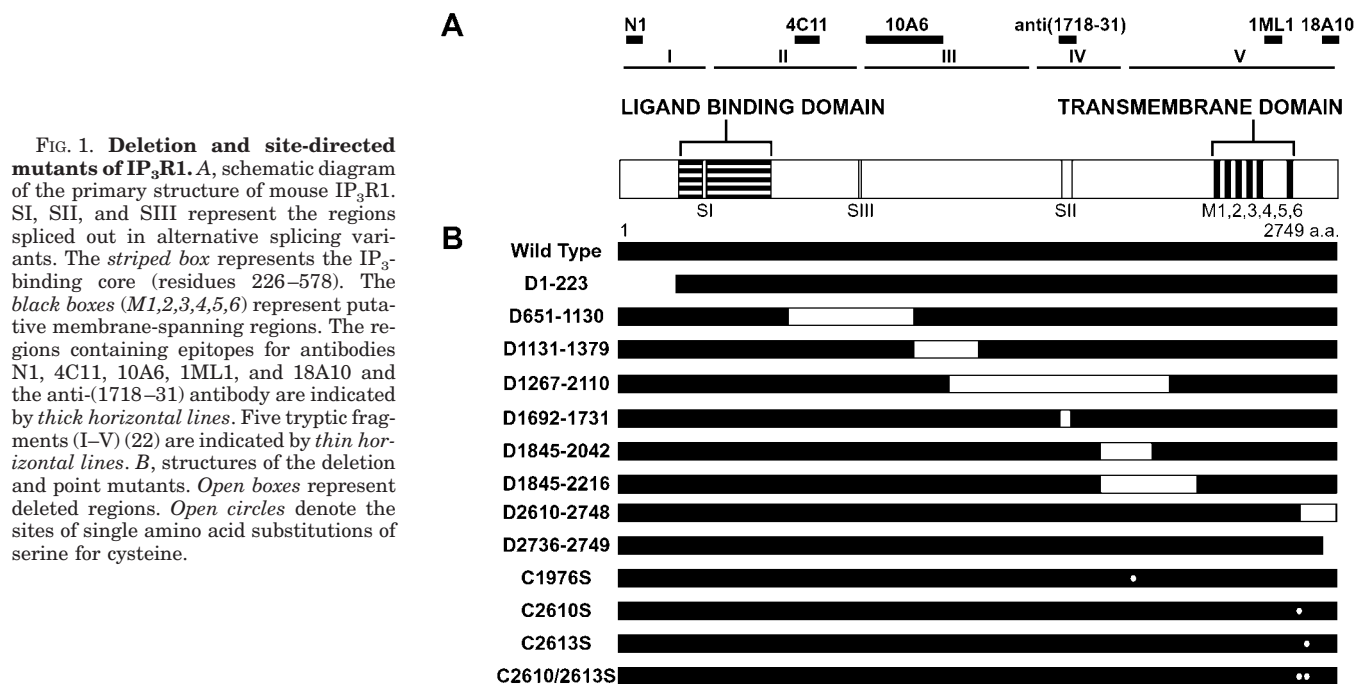
[³H] IP_3 Binding Assay Using Membrane Fractions—The IP_3 binding assay was performed as described previously (6). The membrane fractions (50–200 μ g/tube) were incubated with 9.6 nM [³H] IP_3 (PerkinElmer Life Sciences) in 100 μ l of binding buffer (50 mM Tris-HCl, pH 8.0, 1 mM EGTA, and 1 mM 2-mercaptoethanol) for 10 min at 4 °C. After centrifugation, the pellets were dissolved in Solvable (PerkinElmer Life Sciences), and the radioactivities were measured with a scintillation counter (Beckman LS6500). Nonspecific binding was measured in the presence of 10 μ M unlabeled IP_3 (Dojindo Laboratories).

IICR Assay for Membrane Fractions—The membrane fractions were suspended in Ca^{2+} release buffer supplemented with 1 μ g/ml oligomycin (Sigma), 2 mM $MgCl_2$, 25 μ g/ml creatine kinase (Roche Applied Science), 10 mM creatine phosphate (Sigma), and 2 μ M Fura-2 (Molecular Probes, Inc.) and used at a concentration of 200–300 μ g/ml protein. Fluorescence was recorded at 510 nm with alternate excitation of 340 and 380 nm (F_{340} and F_{380} , respectively). Using a CAF-110 spectrofluorometer (Japan Spectroscopic Co.), signals were recorded every 0.01 s with MacLab Version 3.6 (ADInstruments) at 30 °C. When the Ca^{2+} uptake induced by the addition of 1 mM ATP reached a steady level, 2 μ M thapsigargin was added to eliminate active Ca^{2+} uptake through intrinsic Ca^{2+} pumps. The rate of leakage from the membrane fractions following the addition of thapsigargin was almost linear. When the ratio of fluorescence intensity (F_{340}/F_{380}) reached 1.2, corresponding to ~170 nM free Ca^{2+} , various concentrations of IP_3 were added. At the end of each experiment, 2 mM $CaCl_2$ and 10 mM EGTA were added successively for normalization and calibration (30).

Limited Trypsin Digestion of Mutant Receptors—Limited trypsin digestion was performed as described previously (22). Microsomal fractions (0.25–5 mg/ml) of wild-type and mutant IP_3R1 -expressing cells were incubated with 0.01–10 μ g/ml trypsin in trypsinization buffer (120 mM KCl, 1 mM EDTA, 1 mM 2-mercaptoethanol, and 20 mM Tris-HCl, pH 8.0) at 35 °C for 10 min. The reaction was terminated by the

² Y. Tateishi, M. Hattori, T. Michikawa, M. Iwai, K. Uchida, T. Nakayama, T. Nakamura, T. Inoue, and K. Mikoshiba, unpublished data.

³ H. Miyauchi, K. Uchida, T. Kirino, T. Michikawa, and K. Mikoshiba, manuscript in preparation.



addition of 50 μ g/ml soybean trypsin inhibitor (Sigma) and 0.1 mM phenylmethylsulfonyl fluoride. After the addition of an equal volume of SDS-PAGE sample buffer, reaction mixtures were incubated at 55 $^{\circ}$ C for 30 min. The digested proteins were separated by 8% SDS-PAGE and then analyzed by Western blotting with anti-IP₃R antibodies N1, 4C11, 10A6, 1ML1, and 18A10 and the anti-(1718–31) antibody (see Fig. 1A) (22).

RESULTS

Expression of Deletion Mutants of IP₃R1 in Intrinsically IP₃R-deficient R23-11 Cells—As previously reported (6), we constructed 17 internal deletion mutants of mouse IP₃R1. Among these mutants, we selected seven (Fig. 1B) containing both the IP₃-binding region (residues 226–578) and the putative transmembrane domain (residues 2276–2589) to investigate the critical regions for the coupling between ligand binding and channel opening. In addition, we constructed two mutants lacking residues 1–223 and 2736–2749, respectively (Fig. 1B). To express these mutant receptors, we introduced the mutant cDNAs into R23-11 cells and established stable cell

TABLE I
IP₃-binding properties of the deletion mutants
Values are expressed as means \pm S.D. ($n = 3$).

Recombinant protein	Affinity (K_d) nM	B_{max} pmol/mg protein	Hill coefficient
Wild-type			
KMN13	20 \pm 5	13 \pm 9	1.0 \pm 0.05
KMN107	77 \pm 50	0.77 \pm 0.2	0.97 \pm 0.02
D1-223	1.5 \pm 0.4 ^a	14 \pm 3	1.5 \pm 0.2 ^b
D651-1130	150 \pm 30 ^a	5.2 \pm 3	0.85 \pm 0.1
D1131-1379	12 \pm 1	9.2 \pm 7	1.1 \pm 0.2
D1267-2110	57 \pm 5 ^a	4.2 \pm 1	1.0 \pm 0.04
D1692-1731	22 \pm 6	3.8 \pm 2	0.99 \pm 0.05
D1845-2042	41 \pm 3 ^a	1.7 \pm 0.9	1.0 \pm 0.08
D1845-2216	48 \pm 10 ^a	2.1 \pm 0.5	0.92 \pm 0.02
D2610-2748	67 \pm 50	1.5 \pm 1	1.0 \pm 0.07
D2736-2749	23 \pm 5	7.2 \pm 0.4	0.95 \pm 0.07

^a $p < 0.05$ by Student's t test.

^b $p < 0.01$ by Student's t test.

lines by selection with 2 mg/ml G418. Fig. 2A illustrates the results from Western blot analysis of the membrane fractions prepared from these stable cell lines using anti-IP₃R polyclonal antibody 1ML1, whose epitope lies within residues 2504–2523 of IP₃R1 (Fig. 1A) (10). All of the mutant receptors except D2610–2748 were detected with an appropriate molecular mass (Fig. 2A). Because D2610–2748 was not well recognized by antibody 1ML1, we confirmed the expression of D2610–2748 by Western blot analysis using anti-IP₃R mAb 4C11 (20). As shown in Fig. 2B (open arrowhead), an additional signal with a low molecular mass was detected, indicating that degradation (or truncation) of D2610–2748 occurs in R23-11 cells.

[³H]IP₃-binding Activities of Deletion Mutant IP₃Rs—The IP₃-binding activities of the internal deletion mutant receptors expressed in R23-11 cells were measured by equilibrium [³H]IP₃ binding analysis as described previously (6). There was no significant IP₃-binding activity in the membrane fraction obtained from the R23-11 cells (data not shown). Therefore, we measured the ligand-binding activity of the exogenously expressed IP₃R using membrane fractions obtained from the stable cell lines. The IP₃-binding properties of wild-type and deletion mutant IP₃Rs are summarized in Table I. Wild-type

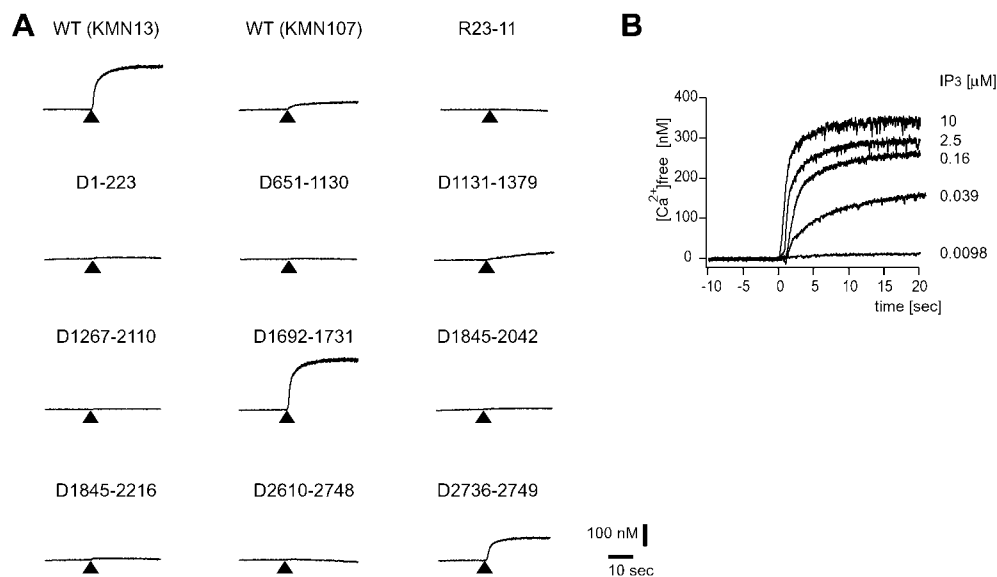


FIG. 3. IP_3 -dependent Ca^{2+} release activity of wild-type and mutant IP_3R1 . *A*, representative time courses of the Ca^{2+} release from the microsomal fractions containing wild-type (WT) and mutant IP_3R1 . Ca^{2+} release was monitored in the presence of 2 μM thapsigargin. IP_3 (10 μM) was added at the times indicated by the arrowheads. Constant leakage (see "Experimental Procedures") was subtracted from each trace. The Ca^{2+} release activity of mutant IP_3R1 was measured in at least three independent experiments. *B*, time courses of Ca^{2+} release through wild-type IP_3R1 following the addition of different IP_3 concentrations. IP_3 was added at time 0.

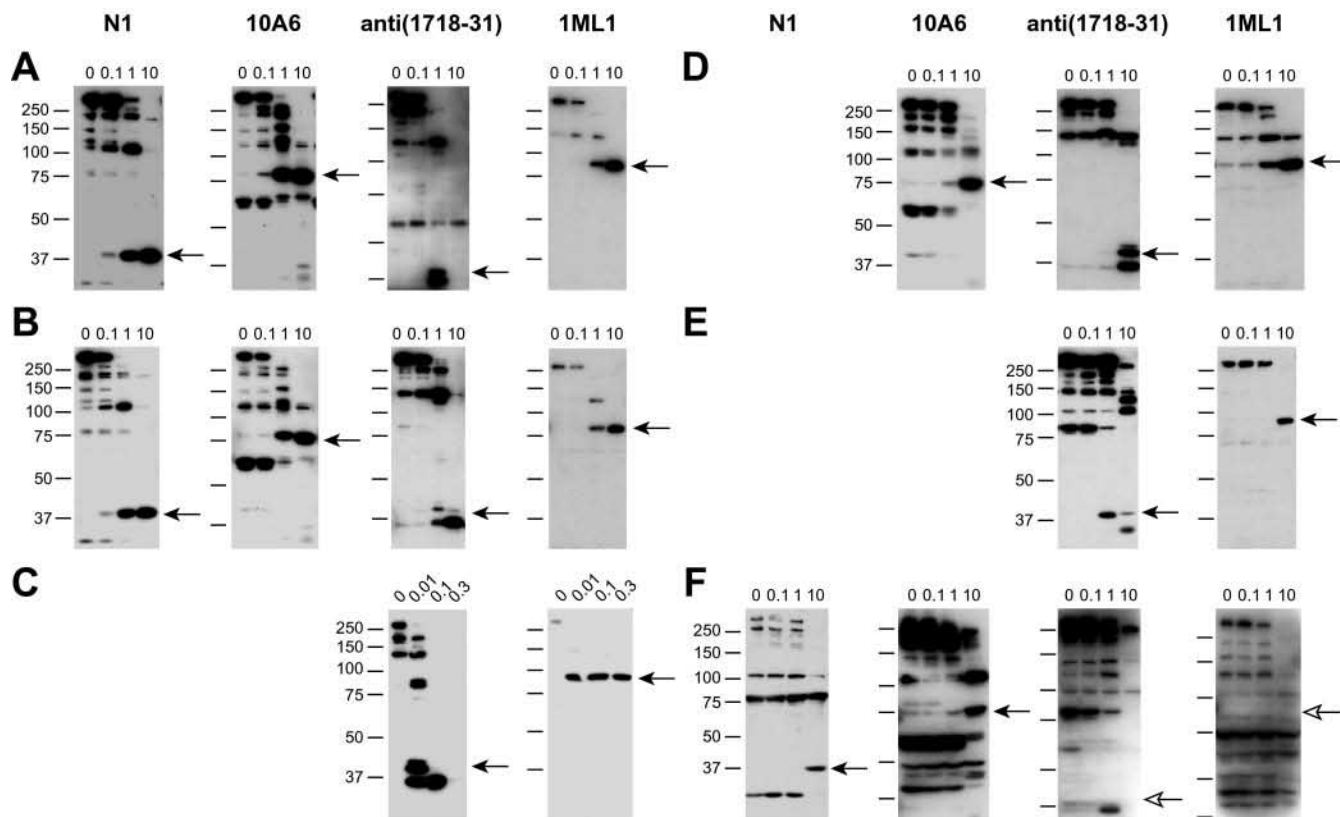



FIG. 4. Fragmentation of wild-type and mutant IP_3R1 by limited trypsin digestion. Crude microsomal fractions (0.25–5 mg/ml protein) were treated with various concentrations of trypsin. Tryptic fragments I and III–V (22) were detected by Western blotting using antibodies N1 and 10A6, the anti-(1718–31) antibody, and antibody 1ML1, respectively. Each major tryptic fragment is indicated by a closed arrow. *A*, wild-type IP_3R1 ; *B*, D2736–2749; *C*, D1131–1379; *D*, D1–223; *E*, D651–1130; *F*, D2610–2748. Trypsin concentrations (micrograms/ml) are indicated above each lane. Molecular mass markers are shown on the left in kilodaltons.

IP_3R1 expressed in R23-11 cells showed a single high affinity IP_3 -binding site with a dissociation constant of 20 ± 5 nM ($n = 3$). This value is close to those of native IP_3R1 expressed in the mouse cerebellum (31) and cDNA-derived IP_3R1 expressed in L cells (28), NG108-15 cells (6), and Sf9 cells (32). Mutant receptors D1131–1379, D1692–1731, D2610–2748, and D2736–2749

exhibited binding affinity similar to that of wild-type IP_3R1 (Table I). The IP_3 -binding affinity of mutant receptors D1267–2110, D1845–2042, and D1845–2216 was 2–3-fold lower (Table I), and mutant D651–1130 had 7.5-fold lower affinity for IP_3 (Table I). Mutant D1–223 exhibited, however, significantly higher affinity for IP_3 (Table I), consistent with a previous



mIP ₃ R1	2590	DTFADLRSEKQKKEEILKTTCTFCIGLERDKFDNKTVTTFEEHIKEEHN	2637
rIP ₃ R1	2590	DTFADLRSEKQKKEEILKTTCTFCIGLERDKFDNKTVTTFEEHIKEEHN	2637
hIP ₃ R1	2536	DTFADLRSEKQKKEEILKTTCTFCIGLERDKFDNKTVTTFEEHIKEEHN	2583
XIP ₃ R	2534	DTFADLRSEKQKKEEVLKTTCTFCIGLERDKFDNKTATFEEHFKEEHN	2581
rIP ₃ R2	2542	DTFADLRSEKQKKEEILKTTCTFCIGLERDKFDNKTVSFEEHIKSEHN	2589
hIP ₃ R2	2542	DTFADLRSEKQKKEEILKTTCTFCIGLERDKFDNKTVSFEEHIKSEHN	2589
rIP ₃ R3	2517	DTFADLRSEKQKKEEILKTTCTFCIGLERDKFDNKTVSFEEHIKLEHN	2564
hIP ₃ R3	2518	DTFADLRSEKQKKEEILKTTCTFCIGLERDKFDNKTVSFEEHIKLEHN	2565
DIP ₃ R	2677	DTFADLRSEKQKKEAILKTTCTFCISLNRSAFDNKTVSFEEHIKSEHN	2724
CIP ₃ R	2717	DTFGDLRAEKNEKEQILKNNCFICGLDRSRFDNRSVTFETHRETHNI	2764
rbRyR1	4938	DAFGELRDQEQVKEDMETKCFICGIGSDYFDTTPHGFETHLLEHN	4985
rbRyR2	4870	DAFGELRDQEQVKEDMETKCFICGIGNDYFDTTPHGFETHLQEHNL	4917
rbRyR3	4773	DAFGELRDQEQVREDMETKCFICGIGNDYFDTTPHGFETHLQEHNL	4820

* : * : * * : : : : : : : : * * * : * * * * * * * :

FIG. 5. Conserved cysteine residues in the C-terminal tail. The C-terminal 48-amino acid sequences next to the transmembrane regions in all three types of IP₃Rs and RyRs are compared. Asterisks and colons indicate identical and similar residues, respectively. Cys²⁶¹⁰ and Cys²⁶¹³ in mouse IP₃R1 are indicated by arrowheads. These amino acid sequences were aligned using the ClustalW algorithm. The GenBank™/EBI Data Bank accession numbers are as follows: mouse IP₃R1 (mIP₃R1), X15373; rat IP₃R1 (rIP₃R1), J05510; human IP₃R1 (hIP₃R1), D26070; *Xenopus* IP₃R (XIP₃R), D14400; rat IP₃R2 (rIP₃R2), X61677; human IP₃R2 (hIP₃R2), D26350; rat IP₃R3 (rIP₃R3), L06096; human IP₃R3 (hIP₃R3), D26351; *Drosophila* IP₃R (DIP₃R), D90403; *Caenorhabditis elegans* IP₃R (CIP₃R), AJ243179; rabbit RyR1 (rbRyR1), X15750; rabbit RyR2 (rbRyR2), U50465; and rabbit RyR3 (rbRyR3), X68650.

report showing that residues 1–223 act as a suppressor for IP₃ binding (12). It has been reported that IP₃ binding to the IP₃R is not cooperative (31, 33), and the same property holds true for the wild-type receptor and all of the mutant receptors except D1–223 expressed in R23-11 cells (Table I). Both the Western blot (Fig. 2) and IP₃ binding (Table I) analyses showed that the amount of IP₃R protein expressed in each cell line was different. The amounts of the mutant IP₃Rs expressed were in the range of 1.5–9.2 pmol/mg of protein (Table I); and therefore, we used two stable cell lines (KMN13 and KMN107)² expressing different amounts of wild-type IP₃R1 as controls in the following experiments. The B_{\max} values for KMN13 and KMN107 were 13 ± 9 and 0.77 ± 0.2 pmol/mg of protein, respectively (Table I).

IICR Activity of Wild-type and Deletion Mutant IP₃Rs—To investigate the Ca²⁺ release activity of the mutant IP₃Rs, IICR from the membrane fractions prepared from each stable cell line was measured in the presence of the Ca²⁺ pump inhibitor thapsigargin. No Ca²⁺ release was observed from membrane fractions prepared from R23-11 cells even after the addition of 10 μ M IP₃ (Fig. 3A), indicating that using R23-11 cells as host cells for transfection allows evaluation of definite Ca²⁺ release activity by exogenously expressed IP₃Rs. Fig. 3B shows the time course of the Ca²⁺ release mediated by recombinant wild-type IP₃R1 after the addition of various concentrations of IP₃. Both the rate and amplitude of Ca²⁺ release depended on the concentration of IP₃ added, indicating that IP₃R1 expressed in R23-11 cells exhibits the quantal Ca²⁺ release that is known to be an intrinsic property of native IP₃R1 (17, 25). As previously reported (11), D1692–1731, which corresponds to the SII[−] alternative splicing variant of IP₃R1 observed in peripheral tissues (34, 35), exhibited Ca²⁺ release after the addition of 10 μ M IP₃ (Fig. 3A). Among the eight artificial mutants (D1–223, D651–1130, D1131–1379, D1267–2110, D1845–2042, D1845–2216, D2610–2748, and D2736–2749), only D1131–1379 and D2736–2749 possessed measurable Ca²⁺ release activity (Fig. 3A). Under the conditions employed, we could detect IICR from membrane fractions prepared from the low level IP₃R1-expressing KMN107 cells (Fig. 3A), which contained 0.77 ± 0.2 pmol of IP₃-binding sites/mg of protein. The expression levels of all the internal deletion mutants in each stable cell line were higher than the expression level of wild-type IP₃R1 in KMN107 cells (Table I). These findings suggest that none of the mutants except D1131–1379 and D2736–2749 act as IP₃-gated Ca²⁺ release channels.

Limited Trypsin Digestion of Mutant IP₃Rs—Mouse cerebellar IP₃R1 is trypsinized into five major fragments (I–V) (Fig. 1A) (22). Limited proteolysis provides direct evidence of protein

TABLE II
IP₃-binding properties of the cysteine mutants
Values are expressed as means \pm S.D. ($n = 3$).

Recombinant protein	Affinity (K_d)	Binding capacity (B_{\max})	Hill coefficient
	nM	pmol/mg protein	
C1976S	27 ± 8	3.0 ± 2	1.1 ± 0.2
C2610S	75 ± 20	1.7 ± 0.5	1.1 ± 0.09
C2613S	36 ± 3	10 ± 7	1.1 ± 0.05
C2610S/C2613S	35 ± 12	3.5 ± 0.7	0.99 ± 0.1

folding (36). To probe the tertiary structure of the mutant IP₃Rs, we analyzed the trypsinized fragments of recombinant IP₃R1. Because R23-11 cells contain an intrinsic mAb 4C11-reactive protein whose molecular mass is similar to that of tryptic fragment II of IP₃R1 (data not shown), we analyzed four tryptic fragments (I and III–V) of the recombinant receptors. As shown in Fig. 4A, wild-type IP₃R1 expressed in R23-11 cells was digested into the same four fragments, indicating that recombinant IP₃R1 retains native structure. We found that trypsin digestion of the Ca²⁺-releasing mutant D2736–2749 generated the same four trypsinized fragments (Fig. 4B), indicating that D2736–2749 folds in the same manner as wild-type IP₃R1. Trypsinization of the other functional mutant, D1131–1379, also generated fragments IV and V (Fig. 4C). However, D1131–1379, which exhibited markedly decreased Ca²⁺ release activity (Fig. 3A), was digested with much lower concentrations of trypsin (Fig. 4C). This difference in trypsin sensitivity suggests that the deletion of amino acids 1131–1379 influences the structure of the C-terminal channel domain. Tryptic fragments of the three functionless mutants, D1–223, D651–1130, and D2610–2748, are shown in Fig. 4 (D–F, respectively). Fragments III–V were generated by trypsin digestion of D1–223 (Fig. 4D). Trypsinization of D651–1130, which lacks a cleavage site between fragments II and III (22), generated fragments IV and V (Fig. 4E). Both D1–223 and D651–1130 exhibited trypsin sensitivity similar to that of wild-type IP₃R1, suggesting that at least the C-terminal channel domains of these mutants fold correctly. By contrast, only fragments I and III were generated by trypsin digestion of D2610–2748 (Fig. 4F), and fragments IV (40 kDa) and V (91 kDa) were not detected (open arrows). These results indicate that deletion of residues 2610–2748 induces a significant distortion of the folding structure of the C-terminal channel domain of IP₃R1.

Identification of the Cysteine Residue Essential for IP₃-induced Gating of IP₃R1—The C-terminal cytoplasmic region following the transmembrane domain has been found to be highly conserved in both the IP₃R and RyR families (13), indi-

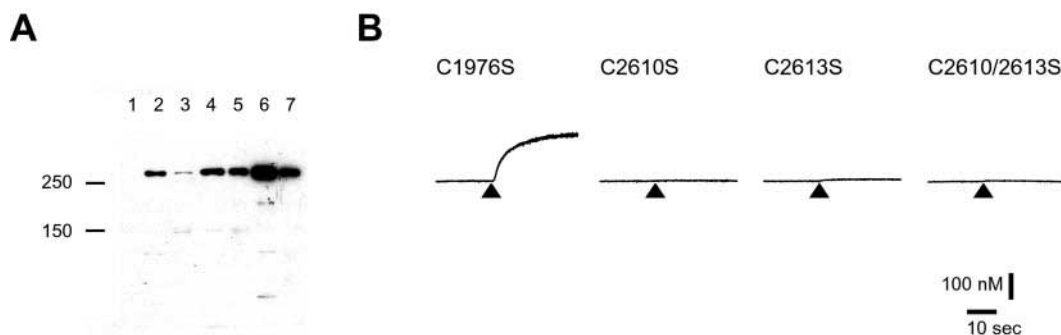


FIG. 6. **Western blot analysis and IP_3 -dependent Ca^{2+} release activity of the cysteine mutants.** A, Western blot analysis of mutants C1976S, C2610S, C2613S, and C2610S/C2613S with antibody 1ML1. Lane 1, R23-11 cells (10 μ g/ml); lane 2, high level wild-type IP_3R -expressing cells (KMN13; 1 μ g); lane 3, low level wild-type IP_3R -expressing cells (KMN107; 10 μ g); lanes 4–7, cells expressing C1976S, C2610S, C2613S, and C2610S/C2613S (10 μ g each), respectively. Molecular mass markers are shown on the left in kilodaltons. B, time courses of the Ca^{2+} release from the microsomal fractions containing cysteine mutants. Ca^{2+} release was monitored in the presence of 2 μ M thapsigargin. IP_3 (2.5 μ M) was added at the times indicated by the arrowheads. Constant leakage was subtracted from each trace.

indicating that this region is involved in the formation of a critical structure that is required for some common functions of the intracellular Ca^{2+} release channels. One of the remarkable features of this region is that it contains two cysteine residues that are conserved in all of the intracellular Ca^{2+} release channels. Both the IP_3R and RyR channels are known to be modified by sulfhydryl reagents (37–39); therefore, we analyzed whether or not the two conserved cysteine residues, Cys²⁶¹⁰ and Cys²⁶¹³ (Fig. 5), are essential for the gating function in mouse IP_3R . We generated three mutant receptors (C2610S, C2613S, and C2610S/C2613S) in which Cys²⁶¹⁰ and/or Cys²⁶¹³ was replaced with serine (Fig. 1B). We also constructed a mutant receptor (C1976S) in which Cys¹⁹⁷⁶ was replaced with serine (Fig. 1B). All of the mutated cDNAs were introduced into R23-11 cells, and stable cell lines expressing mutant receptors were established. Equilibrium [³H] IP_3 binding assay showed that all of the cysteine mutants bound IP_3 with affinities similar to that of wild-type IP_3R (Table II). The expression levels of the mutant receptors were in the range of 1–10 pmol/mg of protein (Table II), and the amounts of all of the mutant receptors expressed in each established cell line were higher than the expression level of wild-type IP_3R in KMN107 cells.

We then examined the Ca^{2+} channel activities of the mutant receptors by measuring IICR from the membrane fractions prepared from the stable cell lines. We found that substitution of serine for Cys²⁶¹⁰ and/or Cys²⁶¹³ completely abolished the Ca^{2+} release activity, whereas no such effect was apparent upon substitution of serine for Cys¹⁹⁷⁶ (Fig. 6). Limited trypsin digestion of C1976S, C2613S, and C2610S/C2613S generated fragments I and III–V (Fig. 7, A, C, and D, closed arrows), indicating that these mutants retain a normal structure. By contrast, trypsin digestion of C2610S generated fragments I, III, and IV (Fig. 7B, closed arrows), but not fragment V (open arrow), indicating that the single amino acid substitution at Cys²⁶¹⁰ induces a significant structural alteration of the C-terminal channel domain of IP_3R .

DISCUSSION

Most cells, including mammalian cultured cells, express two or all three types of the IP_3R (4, 40). Thus, measurement of the actual channel activities of recombinant IP_3Rs in most cells is difficult because of the background activities of the endogenous IP_3Rs . In this study, we used R23-11 cells, which intrinsically lack all of the three IP_3Rs (27), as the host cells to exclude the background effects of the endogenous IP_3Rs . Under the conditions used, neither IP_3 -binding activity nor IP_3 -elicited Ca^{2+} release activity was detected in membrane fractions prepared from R23-11 cells (Fig. 3A). Wild-type IP_3R expressed in

KMN13 cells revealed affinity for IP_3 ($K_d = 20 \pm 5$ nM) (Table I) similar to that of native (31) and recombinant (6, 28, 32) mouse IP_3R and mediated Ca^{2+} release from microsomal vesicles in an IP_3 -dependent manner (Fig. 3B). Wild-type IP_3R expressed in KMN13 cells revealed quantal Ca^{2+} release (Fig. 3B), which is thought to be an intrinsic property of native IP_3Rs (17, 25), suggesting that recombinant IP_3R in R23-11 cells functions properly. Using this system, we determined that six of the mutants investigated in this study, those lacking residues 1–223, 651–1130, 1267–2110, 1845–2042, 1845–2216, and 2610–2748, did not exhibit any measurable Ca^{2+} release activity, whereas the mutants lacking residues 1131–1379 and 2736–2749 retained the activity. [³H] IP_3 binding analysis showed that all of these nonfunctional mutants except D1–223 possessed lower IP_3 -binding affinity (Table I). However, 98.5% of the receptors of even the lowest affinity mutant, D651–1130, whose K_d is 150 nM (Table I), would have been occupied when 10 μ M IP_3 was applied. Therefore, the decrease in IP_3 -binding affinity is unlikely to be the primary cause of the loss of function of these mutants. The limited trypsin digestion of the crude membrane fractions prepared from the mutant-expressing cells showed that not only the IP_3 -gated Ca^{2+} -permeable mutants, D1131–1379 and D2736–2749, but two nonfunctional mutants, D1–223 and D651–1130, generated fragments IV and V (Fig. 4). All of these mutants except D1131–1379 exhibited trypsin sensitivity similar to that of wild-type IP_3R , indicating that these mutants retain a normal folding structure in at least the C-terminal channel-forming domain. Immunocytochemical staining suggested that all of the mutants were localized on the Ca^{2+} stores of the cells (data not shown). Hence, we concluded that at least two regions, *viz.* regions 1–223 and 651–1130, are required for the IP_3 -dependent gating of IP_3R .

The Critical Region 1–223 Is Known as a Suppressor of IP_3 Binding—Deletion of the residues on the N-terminal side of the IP_3 -binding core has a complicated effect on the IP_3 -binding activity (12). A short deletion of the N-terminal 31 residues from the N-terminal 734-amino acid region results in a significant reduction in binding activity even though the mutant includes the entire IP_3 -binding core sequence. Such effects are also found in serial N-terminal deletions up to 215 residues. However, the binding activity recovers when deleted up to the first 220, 223, or 225 amino acids. The mutant lacking the first 223 amino acids shows >10-fold higher affinity for IP_3 than does the parental N-terminal 734-amino acid region. Based on these results, Yoshikawa *et al.* (41) proposed that the first ~225 N-terminal amino acids function as a suppressor of IP_3 binding. In this study, we found that D1–223 had 10-fold higher affinity for IP_3 than did wild-type IP_3R (Table I). In

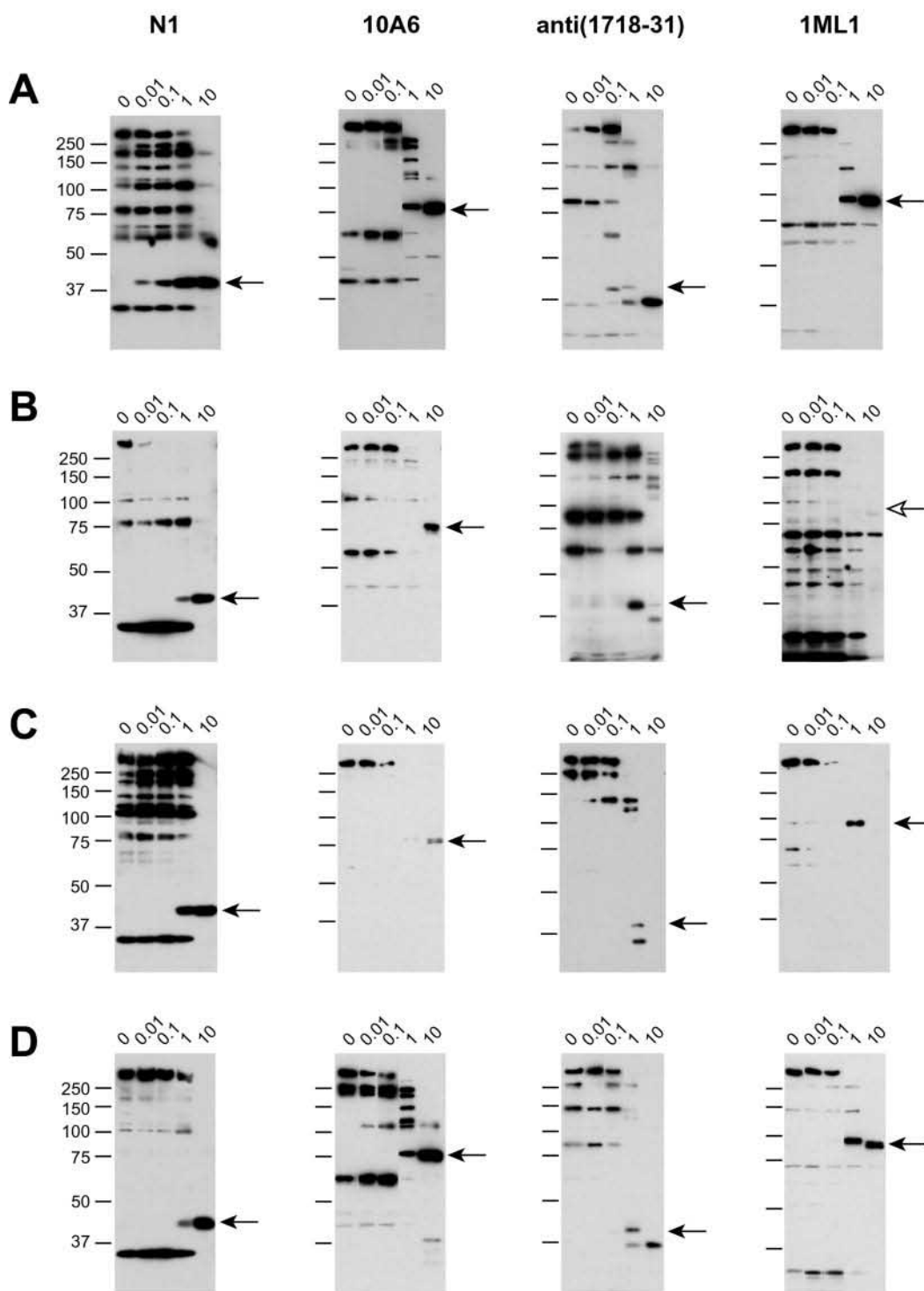


FIG. 7. Limited trypsin digestion of the cysteine mutants of IP_3R1 . Crude microsomal fractions (0.25–5 mg/ml protein) were treated with various concentrations of trypsin. Tryptic fragments I and III–V were detected by Western blotting using antibodies N1 and 10A6, the anti-(1718–31) antibody, and antibody 1ML1, respectively. Each major tryptic fragment is indicated by a closed arrow. *A*, C1976S; *B*, C2610S; *C*, C2613S; *D*, C2610S/C2613S. Trypsin concentrations (micrograms/ml) are indicated above each lane. Molecular mass markers are shown on the left in kilodaltons.

addition, we found that the IP_3 binding of D1–223 was positively cooperative (Table I), indicating that the intersubunit interaction may be elicited (or modified) in the tetrameric complex composed of D1–223. Limited trypsin digestion showed that the mutant is likely to retain the normal folding structure of the C-terminal channel-forming domain (Fig. 4D). Surprisingly, D1–223 did not exhibit any measurable Ca^{2+} release activity (Fig. 3A). These data therefore clearly indicate that

residues 1–223 are required for the functional coupling between IP_3 binding and channel opening.

Homer (42)- and calmodulin (43)-binding sites are localized in region 1–223 of IP_3R1 . Homer forms an adaptor complex that couples between group 1 metabotropic glutamate receptors and IP_3Rs , and it has recently been reported to be capable of associating with RyR1 and up-regulating its Ca^{2+} release activity (44). The Homer-binding motif (PPXXFR) is present in residues

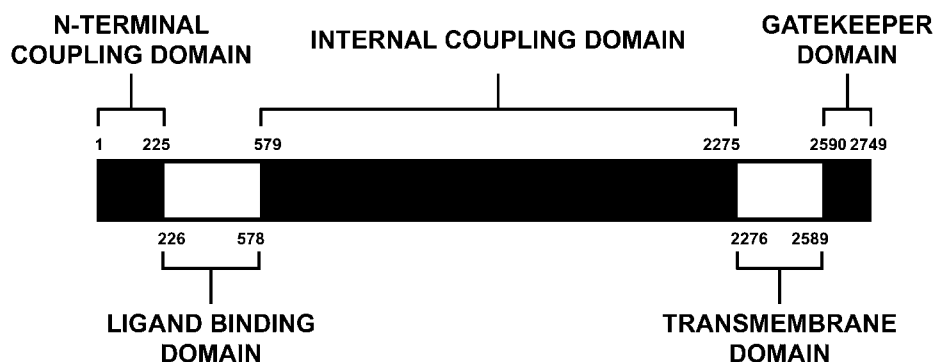


FIG. 8. **Five-domain structure model of IP_3R1 .** In this model, the structure of IP_3R1 is divided into five functional domains, *viz.* an N-terminal coupling domain (residues 1–225), a ligand-binding domain (residues 226–578), an internal coupling domain (residues 579–2275), a transmembrane domain (residues 2276–2589), and a gatekeeper domain (residues 2590–2749). The signal of IP_3 binding is transferred through both the N-terminal and internal coupling domains to the gatekeeper domain, which triggers a conformational change in the activation gate formed within the transmembrane domain.

49–54 (PPKKFR) of mouse IP_3R1 (42). Calmodulin interacts with residues 49–81 and 106–128 in a Ca^{2+} -dependent and Ca^{2+} -independent manner (43). These binding proteins within the critical region 1–223 may modulate the gating of IP_3R1 .

The Critical Region 651–1130 Is Close to the IP_3 -binding Core—In region 651–1130 of IP_3R1 , the alternative splicing site (between amino acids 917 and 918) referred to as SIII is present (45), but the functional significance of the SIII segment (nine residues) has not yet been elucidated. There are three possible Ca^{2+} -binding sites within regions 660–745, 741–849, and 994–1059 (46), suggesting that region 651–1130 is involved in the Ca^{2+} -dependent regulation of IP_3R function. Recently, Bosanac *et al.* (14) unveiled the three-dimensional structure of the IP_3 -binding domain (residues 224–604) that covers the IP_3 -binding core (residues 226–578) of IP_3R1 in the presence of IP_3 . The IP_3 -binding domain forms an asymmetric boomerang-like structure that consists of an N-terminal β -trefoil domain (residues 224–436) and a C-terminal α -helical domain (residues 437–604) containing three armadillo repeat-like folds. IP_3 fits into a cleft formed by these two arms of the boomerang. Our data described here suggest that region 651–1130, which immediately follows the IP_3 -binding core, is essential for IP_3 -induced gating of the channel. What kind of roles does this region have? It is known that other proteins containing armadillo repeats such as β -catenin (47) and importins (48) have >10 repeats. Based on the analysis of the amino acid sequence of IP_3R1 , Bosanac *et al.* (14) suggested that, in IP_3R1 , the armadillo repeat-like folds extend to the C-terminal region of the IP_3 -binding core. It is predicted that many α -helical domains are formed over the entire region 651–1130 (14), and deletion of residues 1131–1379 did not abolish the IP_3 -dependent Ca^{2+} release activity (Fig. 3A). We therefore speculate that the armadillo repeat-like fold-containing α -helical domain, which is essential for IP_3 -induced gating, is formed within residues 440–1130. This region might constitute part of the bridge that connects the IP_3 -dependent conformational change in the IP_3R with channel opening.

Recently, Hamada *et al.* (49) showed that the purified IP_3R from mouse cerebellum contains two distinctive structures: a windmill-like structure and a square-shaped structure. Ca^{2+} reversibly promotes transition from the square- to the windmill-shaped structure, with relocation of the four peripheral IP_3 -binding domains. This observation predicts the presence of a hinge region that changes its conformation drastically following Ca^{2+} binding to the receptor. Hamada *et al.* (49) examined the Ca^{2+} -dependent structural change of the purified IP_3R by limited protease digestion analysis. The results show that a 38-kDa fragment detected using anti- IP_3R1 mAb 4C11 is spe-

cifically generated by cleavage in a solution containing $CaCl_2$, but not in an EDTA-containing solution. The epitope of antibody 4C11 was mapped within residues 679–727 in IP_3R1 (13); and therefore, region 651–1130 found in this study is a strong candidate for the hinge region. The presence of Ca^{2+} -binding sites within this region (46) also supports this hypothesis.

Nonfunctional Mutants D1267–2110, D1845–2042, and D1845–2216—Because the nonfunctional mutants D1267–2110, D1845–2042, and D1845–2216 do not have cleavage sites between tryptic fragments IV and V (Arg¹⁹³¹, Arg¹⁹²³, or Lys¹⁹²⁴) (22), we could not evaluate the folding structure of the C-terminal channel-forming domain of these mutants. Therefore, we did not determine whether the deleted regions include critical regions for activation gating or whether the deletions simply distort the structure of the receptor. Notably, the deleted regions in these mutants include (or are close to) the Ca^{2+} sensor region found in IP_3R1 (50). Cytoplasmic Ca^{2+} is a co-agonist for the IP_3R (51); and thus, the IP_3 - and Ca^{2+} -binding signals must be combined on the IP_3R . More detailed analysis of the regions deleted in these mutants may help us to better understand the molecular mechanism of gating, in particular, the Ca^{2+} -dependent processes during channel opening.

Region 2610–2748 May Be Required for the Correct Folding of IP_3R1 —The C-terminal region following the sixth transmembrane region may play some part in channel gating of the IP_3R because mAbs that recognize this region have been reported to either inhibit (21) or enhance (52) IICR. In addition, it has been suggested that the C terminus is involved in subunit assembly of the IP_3R channel complex (6, 9). It has been shown that, although a truncation mutant of IP_3R1 that lacks all of the transmembrane regions and the succeeding C terminus (amino acids 2218–2749) is present as a monomer, a deletion mutant that lacks only the transmembrane regions (amino acids 2112–2605) forms dimers (6), suggesting that the C-terminal 144 amino acids (positions 2606–2749) are involved in the intersubunit interaction of IP_3R1 . Facilitation of multimer formation of mutant IP_3Rs with two or more transmembrane regions is observed if the mutants are fused to the C-terminal 145 residues (9); however, recombinant IP_3R1 lacking the C-terminal 145 residues forms tetramers (9), suggesting that this C-terminal region is not essential for the formation of the tetrameric channel complex. In this study, we found that deletion of amino acids 2610–2748 completely abolished the activity of the IP_3R channel. D2610–2748 was not well recognized by antibody 1ML1 (Fig. 2A). Limited trypsin digestion of mutant D2610–2748 did not generate tryptic fragments IV and V (Fig. 4F), suggesting that deletion of residues 2610–2748 affects the folding struc-

ture around the cleavage sites between tryptic fragments IV and V.

The Essential Cysteine Residue in the C-terminal Tail—We found that the site-directed mutants C2610S, C2613S, and C2610S/C2613S did not exhibit any measurable Ca²⁺ release activity (Fig. 6). As shown in Fig. 7, limited trypsin digestion of C2613S and C2610S/C2613S generated all four tryptic fragments (I and III–V), whereas trypsinization of C2610S generated only three tryptic fragments (I, III, and IV). These results indicate that Cys²⁶¹³ is required for the functional coupling between IP₃ binding and channel opening. The results of trypsinization of C2610S suggest that substitution of Cys²⁶¹⁰ disrupts the correct folding in at least the C-terminal channel-forming domain of the IP₃R. This is puzzling, however, because C2610S/C2613S generated all four tryptic fragments. The effect of a single amino acid substitution at Cys²⁶¹⁰ could be explained if the cysteine at position 2613 in the C2610S mutant elicits an artificial modification (such as disulfide formation, S-nitrosylation, or palmitoylation) that induces a serious distortion in the folding structure of the C-terminal channel domain. These modifications might be prevented in the presence of Cys²⁶¹⁰. This explanation suggests a direct or indirect structural interaction between Cys²⁶¹⁰ and Cys²⁶¹³ in wild-type IP₃R1.

These cysteine residues are also conserved in the RyR family (Fig. 5). Involvement of the cysteine residues in intracellular Ca²⁺ channel gating has been postulated on the basis of evidence that thiol reagents such as oxidized glutathione and thimerosal enhance the Ca²⁺-mobilizing activity of both IP₃R and RyR channels (1). There are nine cysteine residues conserved in both families (13). As shown in Fig. 6, substitution of the conserved cysteine residue at position 1976 did not affect the activity of IP₃R1, whereas substitution of Cys²⁶¹⁰ or Cys²⁶¹³ caused loss of function of IP₃R1. It is possible that thiol reagents directly attack the cysteine residues at positions 2610 and/or 2613 and enhance channel activity. Further studies are required to elucidate the exact target sites of thiol reagents and the mechanism of the enhancement of channel gating induced by these reagents.

Cysteine residues located in the C-terminal region following the transmembrane domain are known to be involved in the gating of some ion channels on the plasma membrane, such as cyclic nucleotide-gated channels (53–55) and voltage-dependent and inwardly rectifying K⁺ channels (56, 57). In the presence of oxidants, a certain C-terminal cysteine residue in both these plasma membrane channels reacts with a cysteine residue located in the N-terminal region in the same or different subunit. This reaction depends on the states of the channels, and the formation of disulfide bonds results in channel potentiation. On the N-terminal side of the transmembrane domain, the IP₃R possesses 18 cysteine residues that are conserved in the IP₃R family. Thus, examining the interaction between the N and C termini via the formation of disulfide bonds in the presence of some oxidants according to the gating states would be useful in understanding the conformational changes that occur during IP₃R gating.

A Novel Five-domain Structure Model for the IP₃R—We found that two regions, *viz.* regions 1–223 and 651–1130, and Cys²⁶¹³ are crucial for the IP₃-induced gating of IP₃R1. How do they contribute to the activation gating of IP₃R1? Recently, the open pore conformation of K⁺ channels (MthK) was resolved at a resolution of 3.3 Å (58, 59). Structural comparison between KcsA and MthK (closed and open K⁺ channels) revealed that pore-lining inner helices form the channel gate and that bending of the inner helices causes channel opening. In the bent configuration, the inner helices form a wide (12 Å) entryway. The gating hinge is a glycine residue located in the middle of

the inner helices. The glycine residue is highly conserved in voltage- or ligand-gated channels with two or six membrane-spanning segments per subunit, suggesting that the bending of the inner helices is a common mechanism for channel opening. The IP₃R has been proposed to have the same structural arrangement of the pore-forming domain as the voltage-gated K⁺ channels (10); therefore, the IP₃R pore may also be equipped with the same gating mechanism. Pore-lining inner helices that contain the gating hinge in the MthK channel correspond to the sixth membrane-spanning segment of the IP₃R. It is of interest to note that a glycine residue is also present within the sixth membrane-spanning segment of all three types of the IP₃R. This structural similarity suggests that the channel gate is formed by the sixth membrane-spanning helix of the IP₃R. One of the striking differences between the IP₃R and other ligand-gated channels with six membrane-spanning segments, such as cyclic nucleotide-gated channels, is in the location of the ligand-binding site. Both the IP₃-binding site and the Ca²⁺-binding sites are positioned on the N-terminal side of the transmembrane domain of the IP₃R, whereas in other ligand-gated channels, the ligand-binding sites are located in the C-terminal cytoplasmic region that is close to the pore-lining inner helices. In these ligand-gated channels, the ligand-binding signals may be transferred directly to the pore domain and cause bending of the inner helices to open the channels. The ligand-binding signals of the IP₃R may be transferred to the pore domain in a different manner. Based on the results presented here, we propose a novel five-domain structure model in which the C-terminal tail works as a gatekeeper for activation-induced gating of the IP₃R (Fig. 8). In this model, conformational changes in the IP₃-binding domain caused by IP₃ binding are transmitted through both the N-terminal and internal coupling domains to the C-terminal tail, which then triggers channel opening. Cys²⁶¹³ in the C-terminal tail may be critical for receiving the IP₃-binding signal and/or for triggering channel opening. Further studies on the structure and function of the IP₃R using the described experimental approach may provide us with an exact answer for the long-asked question, “How does the binding of IP₃ at the N terminus gate the C-terminal Ca²⁺ permeation pore?”

Acknowledgments—We thank Dr. T. Kurosaki for the kind gift of the DT40 and R23-11 cell lines. We thank Drs. T. Inoue, M. Hattori, A. Mizutani, and K. Hamada for valuable discussions and Drs. A. Miyawaki, H. Mizuno, and C. Hirashima for support and advice during the course of this work. We thank Dr. M. Ikura for critical reading of the manuscript. We also thank Drs. M. Kurosaki and T. Yasuda for assistance with the cell culture technique and helpful discussions. We thank Y. Ueno and M. Iwai for excellent technical assistance. K. U. thanks Drs. N. Matsuo, T. Takahashi, and Y. Kojima for providing this research opportunity.

REFERENCES

- Berridge, M. J. (1993) *Nature* **361**, 315–325
- Maeda, N., Kawasaki, T., Nakade, S., Yokota, N., Taguchi, T., Kasai, M., and Mikoshiba, K. (1991) *J. Biol. Chem.* **266**, 1109–1116
- Furuichi, T., and Mikoshiba, K. (1995) *J. Neurochem.* **64**, 953–960
- Monkawa, T., Miyawaki, A., Sugiyama, T., Yonishima, H., Yamamoto-Hino, M., Furuichi, T., Saruta, T., Hasegawa, M., and Mikoshiba, K. (1995) *J. Biol. Chem.* **270**, 14700–14704
- Südhof, T. C., Newton, C. L., Archer, B. T., III, Ushkaryov, Y. A., and Mignery, G. A. (1991) *EMBO J.* **10**, 3199–3206
- Miyawaki, A., Furuichi, T., Ryou, Y., Yoshikawa, S., Nakagawa, T., Saitoh, T., and Mikoshiba, K. (1991) *Proc. Natl. Acad. Sci. U. S. A.* **88**, 4911–4915
- Joseph, S. K., Boehning, D., Pierson, S., and Nicchitta, C. V. (1997) *J. Biol. Chem.* **272**, 1579–1588
- Sayers, L. G., Miyawaki, A., Muto, A., Takeshita, H., Yamamoto, A., Michikawa, T., Furuichi, T., and Mikoshiba, K. (1997) *Biochem. J.* **323**, 273–280
- Galvan, D. L., Borrego-Diaz, E., Perez, P. J., and Mignery, G. A. (1999) *J. Biol. Chem.* **274**, 29483–29492
- Michikawa, T., Hamanaka, H., Otsu, H., Yamamoto, A., Miyawaki, A., Furuichi, T., Tashiro, Y., and Mikoshiba, K. (1994) *J. Biol. Chem.* **269**, 9184–9189
- Boehning, D., Joseph, S. K., Mak, D. O., and Foskett, J. K. (2001) *Biophys. J.* **81**, 117–124
- Yoshikawa, F., Morita, M., Monkawa, T., Michikawa, T., Furuichi, T., and

- Mikoshiha, K. (1996) *J. Biol. Chem.* **271**, 18277–18284
13. Furuichi, T., Yoshikawa, S., Miyawaki, A., Wada, K., Maeda, N., and Mikoshiha, K. (1989) *Nature* **342**, 32–38
14. Bosanac, I., Alattia, J. R., Mal, T. K., Chan, J., Talarico, S., Tong, F. K., Tong, K. I., Yoshikawa, F., Furuichi, T., Iwai, M., Michikawa, T., Mikoshiha, K., and Ikura, M. (2002) *Nature* **420**, 696–700
15. Yoshikawa, F., Uchiyama, T., Iwasaki, H., Tomomori-Sato, C., Tanaka, T., Furuichi, T., and Mikoshiha, K. (1999) *Biochem. Biophys. Res. Commun.* **257**, 792–797
16. Meyer, T., Wensel, T., and Stryer, L. (1990) *Biochemistry* **29**, 32–37
17. Hirota, J., Michikawa, T., Miyawaki, A., Furuichi, T., Okura, I., and Mikoshiha, K. (1995) *J. Biol. Chem.* **270**, 19046–19051
18. Michikawa, T., Hirota, J., Kawano, S., Hiraoka, M., Yamada, M., Furuichi, T., and Mikoshiha, K. (1999) *Neuron* **23**, 799–808
19. Mignery, G. A., and Südhof, T. C. (1990) *EMBO J.* **9**, 3893–3898
20. Maeda, N., Niinobe, M., Nakahira, K., and Mikoshiha, K. (1988) *J. Neurochem.* **51**, 1724–1730
21. Nakade, S., Maeda, N., and Mikoshiha, K. (1991) *Biochem. J.* **277**, 125–131
22. Yoshikawa, F., Iwasaki, H., Michikawa, T., Furuichi, T., and Mikoshiha, K. (1999) *J. Biol. Chem.* **274**, 316–327
23. Muallem, S., Pandol, S. J., and Beeker, T. G. (1989) *J. Biol. Chem.* **264**, 205–212
24. Meyer, T., and Stryer, L. (1990) *Proc. Natl. Acad. Sci. U. S. A.* **87**, 3841–3845
25. Ferris, C. D., Cameron, A. M., Haganir, R. L., and Snyder, S. H. (1992) *Nature* **356**, 350–352
26. Györke, S., and Fill, M. (1993) *Science* **260**, 807–809
27. Sugawara, H., Kurosaki, M., Takata, M., and Kurosaki, T. (1997) *EMBO J.* **16**, 3078–3088
28. Miyawaki, A., Furuichi, T., Maeda, N., and Mikoshiha, K. (1990) *Neuron* **5**, 11–18
29. Zhang, S., Mizutani, A., Hisatsune, C., Higo, T., Bannai, H., Nakayama, T., Hattori, M., and Mikoshiha, K. (2003) *J. Biol. Chem.* **278**, 4048–4056
30. Grynkiewicz, G., Poenie, M., and Tsien, R. Y. (1985) *J. Biol. Chem.* **260**, 3440–3450
31. Maeda, N., Niinobe, M., and Mikoshiha, K. (1990) *EMBO J.* **9**, 61–67
32. Yoneshima, H., Miyawaki, A., Michikawa, T., Furuichi, T., and Mikoshiha, K. (1997) *Biochem. J.* **322**, 591–596
33. Supattapone, S., Worley, P. F., Baraban, J. M., and Snyder, S. H. (1988) *J. Biol. Chem.* **263**, 1530–1534
34. Nakagawa, T., Okano, H., Furuichi, T., Aruga, J., and Mikoshiha, K. (1991) *Proc. Natl. Acad. Sci. U. S. A.* **88**, 6244–6248
35. Danoff, S. K., Ferris, C. D., Donath, C., Fischer, G. A., Munemitsu, S., Ullrich, A., Snyder, S. H., and Ross, C. A. (1991) *Proc. Natl. Acad. Sci. U. S. A.* **88**, 2951–2955
36. Price, N. C., and Johnson, C. M. (1989) in *Proteolytic Enzymes: A Practical Approach* (Beynon, R. J., and Bonds, J. S., eds) pp. 163–180, IRL Press, Oxford
37. Missiaen, L., Taylor, C. W., and Berridge, M. J. (1991) *Nature* **352**, 241–244
38. Bootman, M. D., Taylor, C. W., and Berridge, M. J. (1992) *J. Biol. Chem.* **267**, 25113–25119
39. Kaplin, A. I., Ferris, C. D., Voglmaier, S. M., and Snyder, S. H. (1994) *J. Biol. Chem.* **269**, 28972–28978
40. De Smedt, H., Missiaen, L., Parys, J. B., Henning, R. H., Sienaeert, I., Vanlingen, S., Gijssens, A., Himpens, B., and Casteels, R. (1997) *Biochem. J.* **322**, 575–583
41. Yoshikawa, F., Iwasaki, H., Michikawa, T., Furuichi, T., and Mikoshiha, K. (1999) *J. Biol. Chem.* **274**, 328–334
42. Tu, J. C., Xiao, B., Yuan, J. P., Lanahan, A. A., Leoffert, K., Li, M., Linden, D. J., and Worley, P. F. (1998) *Neuron* **21**, 717–726
43. Sienaeert, I., Nadif Kasri, N., Vanlingen, S., Parys, J. B., Callewaert, G., Missiaen, L., and De Smedt, H. (2002) *Biochem. J.* **365**, 269–277
44. Feng, W., Tu, J., Yang, T., Vernon, P. S., Allen, P. D., Worley, P. F., and Pessah, I. N. (2002) *J. Biol. Chem.* **277**, 44722–44730
45. Nucifora, F. C., Jr., Li, S. H., Danoff, S., Ullrich, A., and Ross, C. A. (1995) *Mol. Brain Res.* **32**, 291–296
46. Sienaeert, I., Missiaen, L., De Smedt, H., Parys, J. B., Sipma, H., and Casteels, R. (1997) *J. Biol. Chem.* **272**, 25899–25906
47. Huber, A. H., Nelson, W. J., and Weis, W. I. (1997) *Cell* **90**, 871–882
48. Cingolani, G., Petosa, C., Weis, K., and Muller, C. W. (1999) *Nature* **399**, 221–229
49. Hamada, K., Miyata, T., Mayanagi, K., Hirota, J., and Mikoshiha, K. (2002) *J. Biol. Chem.* **277**, 21115–21118
50. Miyakawa, T., Mizushima, A., Hirose, K., Yamazawa, T., Bezprozvanny, I., Kurosaki, T., and Iino, M. (2001) *EMBO J.* **20**, 1674–1680
51. Finch, E. A., Turner, T. J., and Goldin, S. M. (1991) *Science* **252**, 443–446
52. Fadool, D. A., and Ache, B. W. (1992) *Neuron* **9**, 907–918
53. Gordon, S. E., Varnum, M. D., and Zagotta, W. N. (1997) *Neuron* **19**, 431–441
54. Broillet, M. C. (2000) *J. Biol. Chem.* **275**, 15135–15141
55. Rosenbaum, T., and Gordon, S. E. (2002) *Neuron* **33**, 703–713
56. Schulteis, C. T., Nagaya, N., and Papazian, D. M. (1996) *Biochemistry* **35**, 12133–12140
57. Schulte, U., Hahn, H., Wiesinger, H., Ruppertsberg, J. P., and Fakler, B. (1998) *J. Biol. Chem.* **273**, 34575–34579
58. Jiang, Y., Lee, A., Chen, J., Cadene, M., Chait, B. T., and MacKinnon, R. (2002) *Nature* **417**, 515–522
59. Jiang, Y., Lee, A., Chen, J., Cadene, M., Chait, B. T., and MacKinnon, R. (2002) *Nature* **417**, 523–526